Published in final edited form as:
Bioorg Med Chem Lett. 2012 July 15; 22(14): 4532–4535. doi:10.1016/j.bmcl.2012.05.126.

Further optimization of the K-Cl cotransporter KCC2 antagonist ML077: Development of a highly selective and more potent *in vitro* probe

Eric Delpire[a], **Aleksandra Baranczak**[e], **Alex G. Waterson**[b,e], **Kwangho Kim**[e,f], **Nathan Kett**[b,c,d], **Ryan D. Morrison**[b,c,d], **J. Scott Daniels**[b,c,d], **C. David Weaver**[b,f], and **Craig W. Lindsley**[b,c,d,e,*]

[a]Department of Anesthesiology, Vanderbilt University School of Medicine, Nashville, TN 37232, USA

[b]Department of Pharmacology, Vanderbilt University School of Medicine, Nashville, TN 37232, USA

[c]Vanderbilt Center for Neuroscience Drug Discovery, Vanderbilt University School of Medicine, Nashville, TN 37232, USA

[d]Vanderbilt Specialized Chemistry Center for Probe Development (MLPCN), Nashville, TN 37232, USA

[e]Department of Chemistry, Vanderbilt University, Nashville, TN 37232, USA

[f]Vanderbilt Institute of Chemical Biology Synthesis Core, Vanderbilt University School of Medicine, Nashville, TN 37232, USA

Abstract

Further chemical optimization of the MLSCN/MLPCN probe ML077 (KCC2 IC_{50} = 537 nM) proved to be challenging as the effort was characterized by steep SAR. However, a multidimensional iterative parallel synthesis approach proved productive. Herein we report the discovery and SAR of an improved novel antagonist (VU0463271) of the neuronal-specific potassium-chloride cotransporter 2 (KCC2), with an IC_{50} of 61 nM and >100-fold selectivity versus the closely related Na-K-2Cl cotransporter 1 (NKCC1) and no activity in a larger panel of GPCRs, ion channels and transporters.

Keywords

Potassium-chloride co-transporter 2; KCC2; NKCC1; antagonist

Due to their key regulatory roles in CNS physiology, cation-chloride cotransporters, and in particular, the neuronal specific K-Cl cotransporter 2 (KCC2) has recently garnered a great deal of attention[1–4]. KCC2, identified in 1996,[5] modulates inhibitory neurotransmission in both the brain and spinal cord.[6–11] However, due to a complete lack of selective and potent

*To whom correspondence should be addressed: craig.lindsley@vanderbilt.edu.

pharmacological tools,[4] the study of KCC2 has relied on either high doses of furosemide or genetic models (mouse and *Drosophila* knockout or transgenic zebrafish).[1–4,12–15] Based on the necessity of small molecule probes to dissect the role of KCC2, an HTS compatible screen in 384-well plates was developed based on thallium (Tl^+ flux) in KCC2-overexpressing HEK293 cells.[4,16] Under the auspice of the MLSCN/MLPCN, 234,560 compounds were screened against KCC2, and after obligate counter- and secondary screens, 26 hits were identified as KCC2 antagonists.[4] Of these, VU0240511 (**1**) emerged as an attractive, potent hit (KCC2 IC_{50} = 568 nM), with >100-fold selectivity versus Na-K-2Cl cotransporter 1 (NKCC1), a critical anti-target as inhibition leads to ototoxic effects (Fig. 1). Upon profiling in an ancillary pharmacology panel of 68 GPCRs, ion channels and transporters, **1** showed significant inhibition (>50% @ 10 μM) of several GPCRs and key ion channels (hERG and L-Type Ca^{2+} channels). Based on similar issues in the past, we converted the secondary amide in **1** to a tertiary *N*-Me amide, VU0255011 (**2**). While **2** displayed a slight improvement in KCC2 potency (KCC2 IC_{50} = 537 nM) and maintained >100-fold selectivity versus NKCC1, we were gratified to note a cleaner ancillary pharmacology profile (no activities >50% @ 10 μM).[4] Thus, **2** was declared an MLSCN/MLPCN probe and given the designation ML077.[17] As such, ML077 is freely available upon request,[18] and we have supplied ML077 to multiple laboratories around the world. While good data is being generated, there is a need for a more potent KCC2 antagonist. In this Letter, we detail the DMPK characterization of ML077 and the further chemical lead optimization of ML077 en route to a more potent *in vitro* KCC2 antagonist probe.

In the pilot phase of the Molecular Libraries initiative,[17] coined the MLSCN, DMPK profiling of probes was not supported. Now in the production phase, or MLPCN, DMPK profiling is required.[18] Thus, prior to further optimization, we profiled ML077 in an effort to assess disposition. In our tier 1 *in vitro* DMPK screen, compound ML077 displayed no significant P450 inhibition in human liver microsomes (IC_{50} >30 μM vs. 3A4, 2C9, 1A2 and ~24 μM inhibition of 2D6) and high plasma protein binding with fraction unbound (f_u) levels between 1 and 2% in rat and human plasma, respectively. Intrinsic clearance (CL_{int}) determined in rat and human liver microsomes indicated that compound ML077 was rapidly cleared *in vitro* (rat, CL_{int} = 294 mL/min/kg; human, CL_{int} = 228.9 mL/min/kg). An *in vitro* to *in vivo* correlation (IVIVC) was established, as ML077 was found to be a highly cleared compound in rat (CL = 185 mL/min/kg) following intravenous administration (1 mg/kg); the high volume of distribution at steady state (Vss 5.0 L/kg) and super-hepatic clearance produced a relatively short $t_{1/2}$ (26 min) *in vivo*. Thus, to deliver an *in vivo* KCC2 probe, significant improvements in the DMPK profile are required. Note, however, that despite a poor PK, ML077 was used successfully to block KCC2 in spinal cord through intrathecal injection.[11]

The initial chemical optimization plan for ML077, utilizing multi-dimensional iterative parallel synthesis,[19] is detailed in Figure 2, and the synthesis of analogs of ML077 was performed as shown in Scheme 1. Various heteroaryl amines **3** (1° and 2°) are treated with α-chloroacetyl chloride **4** (or α-alkyl substituted variants) to deliver functionalized α-chloroamides **5**. Commercially available heteroaryl and heterobiaryl chlorides **6** are treated with thiourea under microwave-assisted conditions to produce the corresponding thiols **7**. Finally, reaction of α-chloroamides **5** with thiols **7** in the presence of Cs_2CO_3 affords a diverse array of analogs **8** of ML077.

Analogs **8** were screened at both 20 μM and 2 μM concentrations prior to full CRCs in an ^{86}Rb uptake assay. SAR was incredibly steep, with the majority of analogs **8** affording <20% inhibition at 20 μM. Functionalization at any position of the western 6-phenyl moiety of ML077 with small alkyl groups, alkoxy groups or halogens was not tolerated. Similarly, replacements for the pyridazine (pyridines, pyrazines, pyrimidines and thiadiazoles) were

also not tolerated, with the exception of two weak, 2-pyridyl-based KCC2 antagonists **9** and **10** (Fig. 3). Moreover, alternative substitutions to the eastern thiazole or alternative heterocycles (pyridines, pyrazine, pyrimidines, etc…) to replace the thiazole were inactive.

Thus, an unsubstituted 6-phenyl pyridazine, in combination with the 4-methyl thiazole, was required for KCC2 inhibition. Therefore, we focused on incorporating larger alkyl and cycloalkly moieties to replace the tertiary *N*-Me amide in **2** (Fig. 2), as well as exploring the impact of simple alkyl substitution α-to the amide (Table 1).[19] For the latter, we first evaluated the racemic mixture, and then resolved, by chiral SFC, and assayed the single enantiomers.[19] This effort was far more productive, affording KCC2 antagonists **11** with improved potency relative to **2**, and the first examples of enantioselective KCC2 inhibition. **11a–d** employed either *N*-Me or *N*-Et tertiary amides with a racemic α-Me or α-Et moiety, and these analogs showed weak KCC2 inhibition (27–57%@2μM). When the steric bulk of the tertiary amide was increased to an *N*-cyclopropyl moiety, KCC2 inhibitory activity was improved. The racemic α-Me congener **11e** and the α-Et derivative **11h** displayed IC_{50}'s of 570 nM and 756 nM, respectively, comparable to **2**. Chiral SFC resolution of the single enantiomers of **11e** afforded **11f**, the (+)-enantiomer, and **11g** the (−)-enantiomer. Here, the (+)-enantiomer **11f** is a potent KCC2 antagonist (IC_{50} = 152 nM), while the (−)-enantiomer **11g** is ~10-fold less active (IC_{50} = 1900 nM). A similar enantiopreference is observed with the α-ethyl congeners **11i** and **11j**. These data represent the first example of enantiospecific inhibition of KCC2. Based on the impact of the *N*-cyclopropyl amide, we then surveyed this modification with an unsubstituted core, affording **11k**, the most potent KCC2 antagonist reported to date (IC_{50} = 61 nM).[19] As we further increased the steric bulk of the tertiary amide to *N*-cyclobutyl, **11m** (IC_{50} = 177 nM), and *N*-cyclopentyl, **11n** (IC_{50} = 1057 nM), KCC2 potency diminished (Table 1). Based on these data, efforts focused on the further characterization of **11k** (VU0463271).

Figure 4 displays the full dose-response curves for both **2** (ML077) and **11k** (VU0463271) for both KCC2 and NKCC1, our standard anti-target in ^{86}Rb uptake assays.[4] Here, both **2** (IC_{50} = 537 nM) and **11k** (IC_{50} = 61 nM) are potent KCC2 antagonists, but only display weak, partial inhibition of NKCC1 function at concentrations up to 100 μM. In the Lead Profiling screen at Ricerca (68 GPCRs, ion channels and transporter radioligand binding assays),[21] **11k** displayed no significant activities (no inhibition >50%@10 μM). Thus, **11k** is ~9-times more potent than ML077, and maintains an excellent ancillary pharmacology profile. In our tier 1 *in vitro* DMPK screen, compound **11k** displayed only very P450 inhibition in human liver microsomes (IC_{50} >30 μM vs. 3A4, 2C9, 2D6 and ~20 μM inhibition of 1A2). Plasma protein binding, with fraction unbound (f_u) levels, could not be determined for 11k, as it was found to be unstable in rat plasma (6% remaining after 1 hour at 37 °C). Intrinsic clearance (CL_{int}) determined in human liver microsomes indicated that compound **11k** was rapidly cleared *in vitro*, and was found to be a moderate-to-high clearance compound in rat (CL = 57 mL/min/kg) following intravenous administration (1 mg/kg); the low volume of distribution at steady state (Vss 0.4 L/kg), coupled with moderate-to-high clearance produced a relatively short $t_{1/2}$ (9 min) *in vivo*. Thus, to deliver an *in vivo* KCC2 probe, significant improvements in the DMPK profile are still required. However, **11k** represents a significant improvement in terms of an *in vitro* KCC2 antagonist probe relative to ML077.

Based on the steep SAR and poor *in vivo* PK, we elected to revisit our HTS hits in an effort to develop an *in vivo* KCC2 antagonist probe. Very few hits from the HTS showed reasonable KCC2 potency in conjunction with NKCC1 selectivity; however, dihydropyrimidine dione **12** (IC_{50} = 640 nM) and [1,2,3]triazolo[4,5-*d*]pyrimidine **13** (IC_{50} = 1.2 μM) represented acceptable starting points (Fig. 5). Similar multidimensional iterative parallel synthesis approaches for the lead optimization of **12** and **13** led to inactive

compounds once again. Recognition of the structural similarities between **12**, **2** and **11k** led us to generate chimeras, replacing the dihydropyrimidine dione of **12** with the 4-methyl thiazole moiety found in **2** and **11k** and a number of other azaheterocycles. However, all the chimeras were inactive or very weak inhibitors (IC_{50}'s >20 μM) of KCC2.

In summary, we have further optimized the KCC2 antagonist probe ML077, by application of a multi-dimensional iterative parallel synthesis approach, to afford **11k** (VU0463271), the most potent (KCC2 IC_{50} = 61 nM) and selective (>100-fold versus NKCC1 and inactive in an ancillary pharmacology panel of 68 GPCRs, ion channels and transporters) KCC2 antagonist reported to date. While possessing a favorable *in vitro* DMPK profile, **11k** is a highly cleared, short half-life compound not suitable as an *in vivo* probe. Attempts to optimize additional HTS hits, including chimeras with **11k**, were not productive. Overall, the SAR of all the KCC2 antagonist series was extremely steep. At present, the MLPCN screening deck has more than doubled since the KCC2 screen was originally performed, and we are actively pursuing a rescreen to identify more tractable hits with the potential to develop an *in vivo* probe to compliment our *in vitro* KCC2 probe **11k**. As both ML077 and **11k** were developed for the MLPCN, they are freely available upon request. Additional refinements and studies are in progress and will be reported in due course.

Acknowledgments

The authors acknowledge Emily Days and Christopher Farmer of the Vanderbilt High Throughput Screening facility and the legacy MLSCN Screening Center for GPCRS, ion channels and transporters. This work was supported by grants from the NIH. Vanderbilt is a Specialized Chemistry Center within the Molecular Libraries Probe Centers Network (U54MH84659).

References

1. Woo N-S, Lu J, England R, McClellan R, Dufour S, Moint DB, Deutch AY, Lovinger DM, Delpire E. Hippocampus. 2002; 12:258–268. [PubMed: 12000122]
2. Zhu L, Polley N, Mathews GC, Delpire E. Epilepsy Res. 2008; 79:201–212. [PubMed: 18394864]
3. Morgado C, Pinto-Ribeiro F, Tavares I. Neurosci. Lett. 2008; 438:102–106. [PubMed: 18457921]
4. Delpire E, Days E, Lewis LM, Mi D, Kim K, Lindsley CW, Weaver CD. Proc. Natl. Acad. Sci. USA. 2009; 106:5383–5388. [PubMed: 19279215]
5. Payne JA, Stevenson TJ, Donaldson LF. J. Biol. Chem. 1996; 271:16245–16252. [PubMed: 8663311]
6. Nomura H, Sakai A, Umino M, Suzuki H. Neurosci, Res. 2006; 56:435–440. [PubMed: 17007947]
7. Jolivalt CG, Lee CA, Ramos KM, Calcutt NA. Pain. 2008; 140:48–57. [PubMed: 18755547]
8. Miletic G, Miletic V. Pain. 2008; 137:532–539. [PubMed: 18063479]
9. Zhang W, Liu L-Y, Xu TL. Neuroscience. 2008; 152:502–510. [PubMed: 18262726]
10. Cramer SW, Baggott C, Cain J, Tilghman J, Allcock B, Miranpuri G, Rajpal S, Sun D, Resnicj D. Mol. Pain. 2008; 4:36. [PubMed: 18799000]
11. Austin TM, Delpire E. Anesth. Analg. 2011; 113:1509–1515. [PubMed: 21965363]
12. Hubner CA, Stein V, Hermans-Borgmeyer I, Meyer T, Ballanyl K, Jentsch TJ. Neuron. 2001; 30:515–524. [PubMed: 11395011]
13. Zhu L, Lovinger D, Delpire E. J. Neurophysiol. 2005; 93:1557–1568. [PubMed: 15469961]
14. Hekmat-Scafe DS, Lundy MY, Ranga R, Tanouye MA. J. Neurosci. 2006; 26:8943–8954. [PubMed: 16943550]
15. Reynolds A, Brustein E, Liao M, Mercado A, Babilonia E, Mount DB, Drapeau P. J. Neurosci. 2008; 28:1588–1597. [PubMed: 18272680]
16. Weaver CD, Harden D, Dworetzky SI, Robertson B, Knox RJ. J. Biomol. Screen. 2004; 9:671–677. [PubMed: 15634793]
17. For information on the MLI or MLPCN please see: http://mli.nih.gov/mli/mlpcn/

18. To request your free sample of ML077 or **11k**, please email: craig.lindsley@vanderbilt.edu
19. Kennedy JP, Williams L, Bridges TM, Daniels RN, Weaver CD, Lindsley CW. J. Combi. Chem. 2008; 10:345–354.
20. Experimental details and characterization data for compounds in Table 1. Synthesis of **11k**: To a solution of cyclopropyl-(4-methyl-thiazol-2-yl)-amine (160 mg, 1 mmol) (117 mg, 1 mmol, 82.5 μL) and chloroacetyl chloride (117 mg, 1 mmol, 82.5 μL) in CH_2Cl_2 (3.4 mL, 0.3 M) at 0 °C was added Et_3N (104 mg, 1 mmol, 144 μL). After 30 min, complete consumption of starting material as followed by liquid chromatography-mass spectrometry (LC-MS) was observed. Saturated, aqueous solution of NH_4Cl was added. The aqueous layer was extracted with CH_2Cl_2 (× 2). The combined organic layers were dried ($MgSO_4$), filtered, and concentrated in vacuo. The residue was taken to the next step without further purification. To a solution of 6-phenylpyridazine-3-thiol (214 mg, 1.14 mmol) and 2-chloro-*N*-cyclopropyl-N-(4-methylthiazol-2-yl)acetamide (~1 mmol) in CH_3CN (5 mL, 0.2 M) at ambient temperature was added Cs_2CO_3 (506 mg, 1.55 mmol). After 18 h the reaction mixture was diluted with EtOAc and washed with H_2O (× 2). The organic layer was dried ($MgSO_4$), filtered and concentrated in vacuo. The residue was purified by flash chromatography (Hexane/EtOAc, 4:1) to provide desired product as a yellow oil (216 mg, 56% over two steps). ^{1}H NMR (400 MHz, $CDCl_3$): δ 7.99 (d, J = 1.6 Hz, 1 H), 7.97 (s, 1 H), 7.64 (d, J = 9.2 Hz, 1 H), 7.48-7.45 (m, 4 H), 6.59 (s, 1 H), 4.80 (s, 2 H), 3.31-3.28 (m, 1 H), 2.38 (s, 3 H), 1.28 (m, 2 H), 1.01 (m, 2 H); ^{13}C NMR (100 MHz, $CDCl_3$): δ 169.4, 160.2, 159.0, 156.5, 147.5, 135.9, 129.8, 128.9, 126.6, 126.2, 123.4, 110.3, 34.8, 30.5, 17.4, 11.3; HRMS (ESI) calcd for $C_{19}H_{19}N_4OS_2$ [M+H+] 383.1000 found 383.1000. Characterization of **11e–g** ^{1}H NMR (400 MHz, CDCl3): δ 8.01 (d, J = 2.0 Hz, 1 H), 7.99 (d, J = 1.6 Hz, 1 H), 7.65 (d, J = 9.2 Hz, 1 H), 7.51-7.48 (m, 3 H), 7.37 (d, J = 9.2 Hz, 1 H), 6.60 (s, 1 H), 6.05 (bs, 1 H), 3.33 (bs, 1 H), 2.36 (s, 3 H), 1.77 (d, J = 6.8 Hz, 3 H), 1.24-1.18 (m, 2 H), 1.10-1.05 (m, 1 H), 0.90-0.86 (m, 1 H); ^{13}C NMR (100 MHz, $CDCl_3$): δ 173.7, 160.3, 159.1, 156.6, 147.6, 135.8, 129.9, 129.0, 128.9, 127.7, 126.6, 126.2, 123.5, 110.5, 40.86, 30.68, 18.59, 17.44; HRMS (ESI) calcd for $C_{20}H_{21}N_4OS_2$ [M +H+] 397.1154 found 397.1157. Peak A $[\alpha]_D^{20}$ +290.3° (c = 0.033, $CHCl_3$) SFC preffered column: chiralpak ia RT = 2.23 min; Peak A $[\alpha]_D^{20}$ −296.0° (c = 0.036, $CHCl_3$) SFC preferred column: chiralpak ia RT = 2.79 min. Experimental details for the KCC2-overexpressing HEK293 cells and for ^{86}Rb uptake experiments can be found in reference 4.
21. For full information on the targets in the Lead Profiling Screen at Ricerca, please see: www.ricerca.com

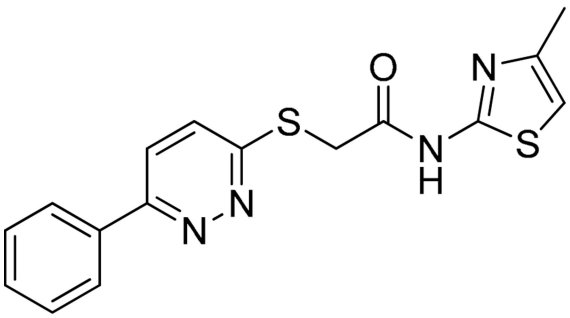

1, VU0240511
KCC2 IC_{50} = 568 nM
NKCC1 IC_{50} > 50 μM
4 significant hits in Ricerca panel

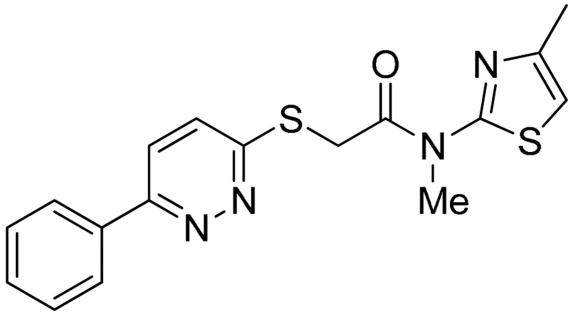

2, VU0255011 (ML077)
KCC2 IC_{50} = 537 nM
NKCC1 IC_{50} > 50 μM
No hits in Ricerca panel

Figure 1.
Structures of the KCC2 antagonist HTS hit (**1**) and the KCC2 antagonist MLPCN probe (**2**), ML077. Simple conversion to the tertiary *N*-Me amide eliminated all ancillary pharmacology while maintaining KCC2 potency and selectivity.

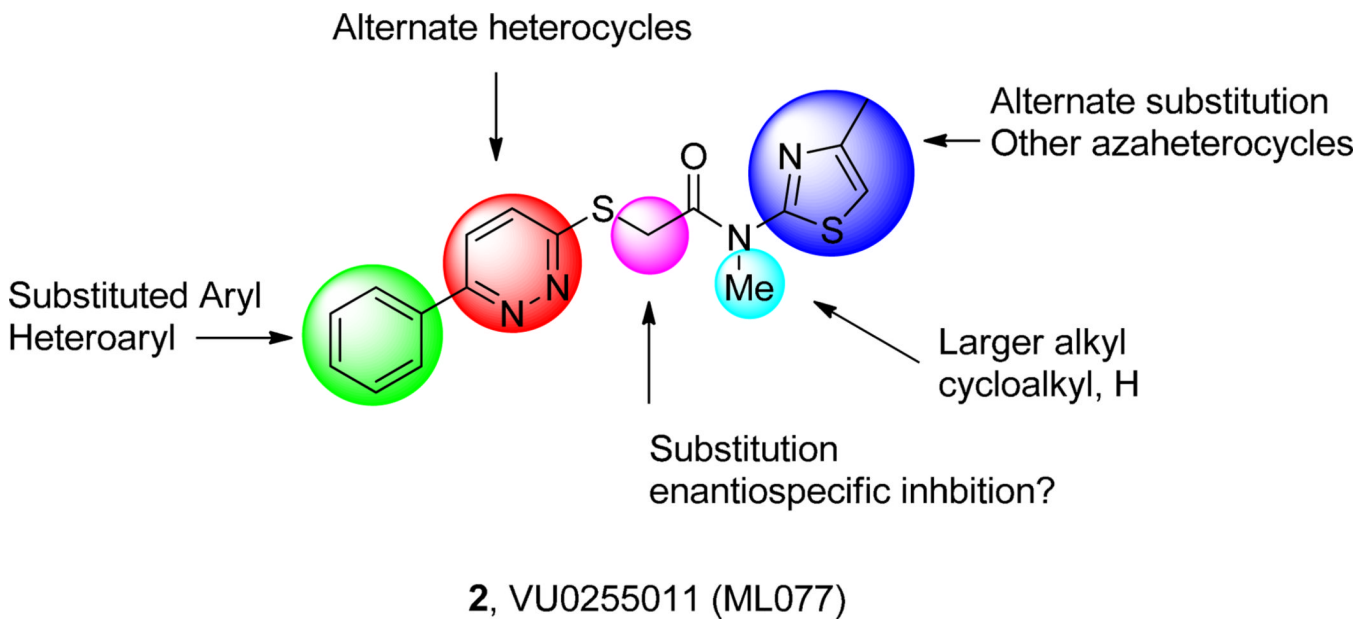

2, VU0255011 (ML077)

Figure 2.
Initial chemical optimization plan for ML077 to improve KCC2 potency.

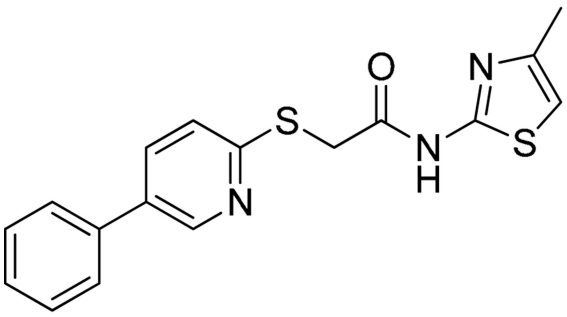

9

KCC2 IC_{50} = 6.9 μM

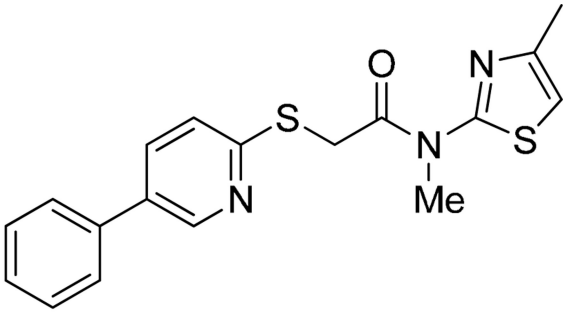

10

KCC2 IC_{50} = 2.9 μM

Figure 3.
2-Pyridyl-based weak KCC2 antagonists **9** and **10** from first generation libraries.

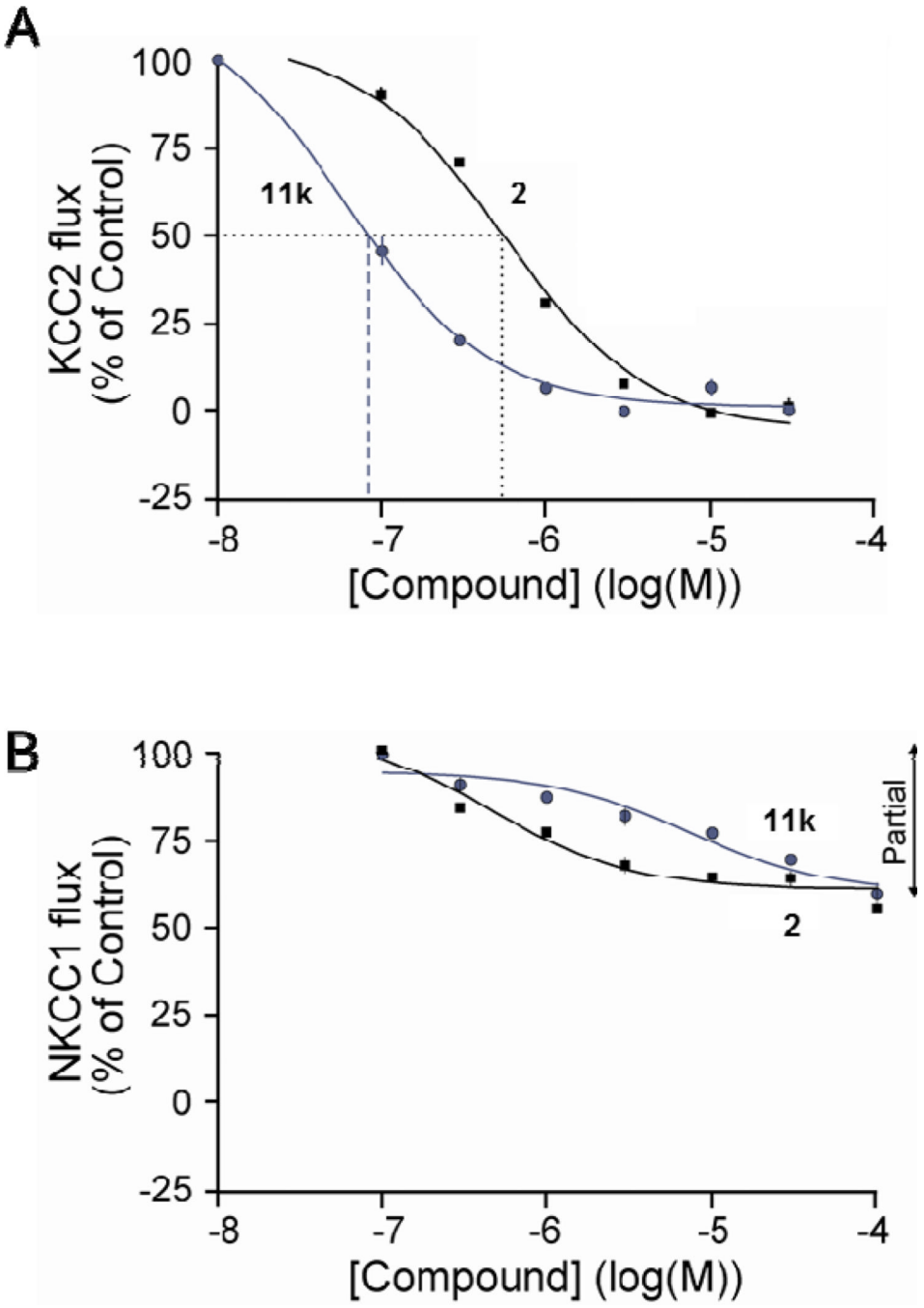

Figure 4.

Dose-response curves for **2** (ML077) and **11k** (VU0463271). A) Full dose-response curves for **2** and **11k** on KCC2 function in an ^{86}Rb uptake assay, highlighting the increased potency of **11k** versus the original probe ML077 (**2**). B) Full dose-response curves for **2** and **11k** on NKCC1 function in an ^{86}Rb uptake assay, with both displaying weak partial inhibition at concentrations up to 100 μM.

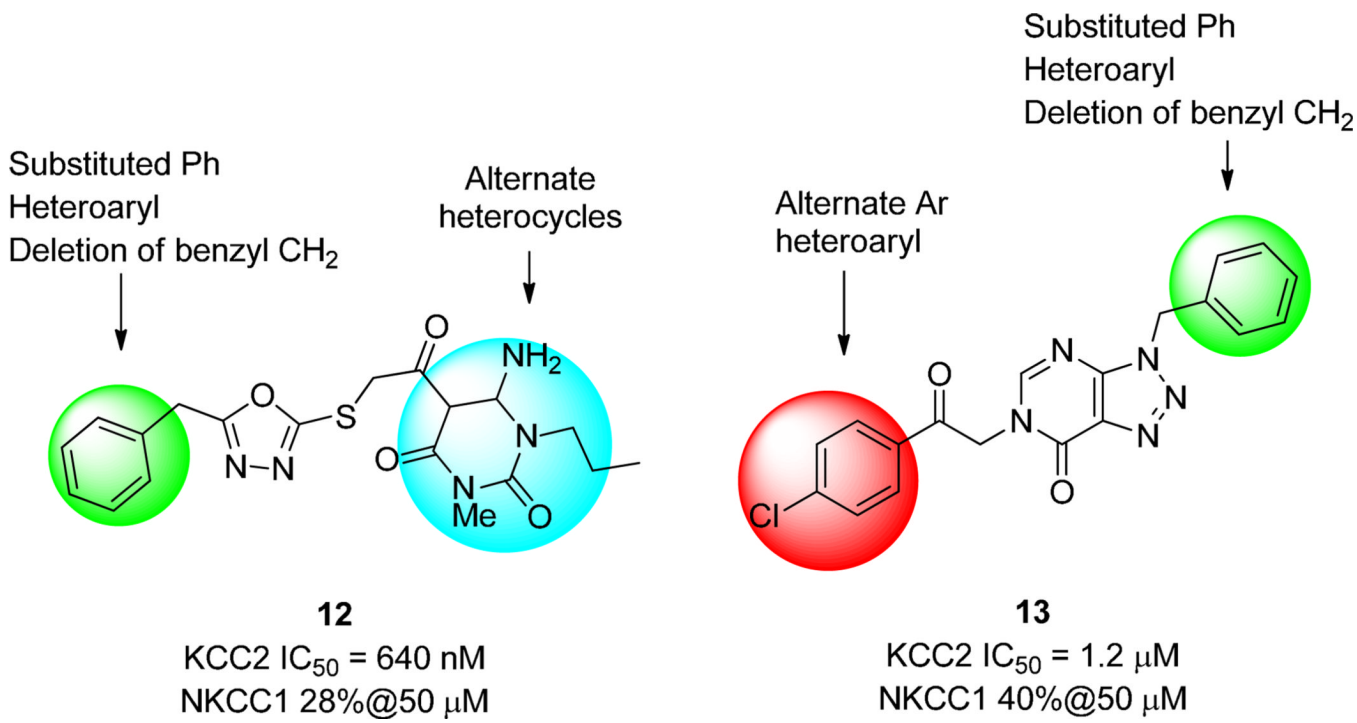

Figure 5.
Structures of the KCC2 antagonist HTS hits **12** and **13**, with selectivity versus NKCC1, and the multi-dimensional iterative parallel synthesis approach for their chemical optimization.

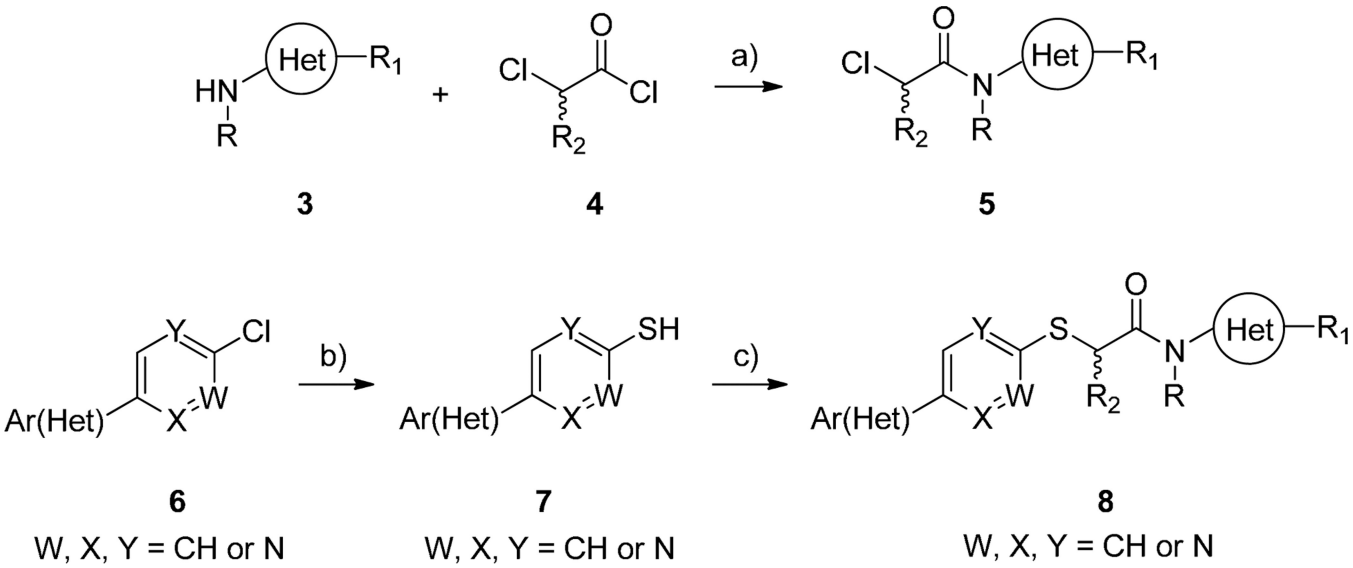

Scheme 1.

Reagents and conditions: (a) Et_3N, CH_2Cl_2, 0 °C, 65–95%; (b) thiourea, 220 °C, microwave, 15 min, 70–85%; (c) Cs_2CO_3, CH_3CN, rt, 56–80%.

Table 1

Structures and activities of analogs **11**.

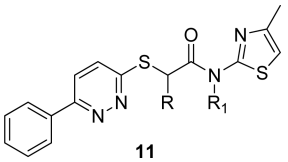

11

Cmpd	R	R_1	% Inhib. @ 2 μM	IC_{50} (nM)
2	H	Me	82	537
11a	(±)-Me	Me	46	ND
11b	(±)-Et	Me	27	ND
11c	(±)-Et	Et	45	ND
11d	(±)-Me	Et	57	ND
11e	(±)-Me		87	570
11f	[a](±)-Me		ND	152
11g	[a](−)-Me		ND	1,900
11h	(±)-Et		84	756
11i	[a](+)-Et		ND	385
11j	[a](−)-Et		40	ND
11k	H		ND	61
11m	H		ND	177
11n	H		ND	1057

ND: not determined.

[a]enantiomers separated by chiral SFC and (+) or (−) rotation noted,[19] absolute stereochemistry is unknown.